JOURNAL OF MATERIALS SCIENCE 35 (2000) 1379–1388

Strength differential effect in four commercial steels

A. P. SINGH, K. A. PADMANABHAN*, G. N. PANDEY†, G. M. D. MURTY, S. JHA
Reserch and Development Centre for Iron and Steel, Steel Authority of India Limited, Ranchi-834 002, India

The difference between compressive and tensile flow stress of a material at a given strain termed as strength differential (S-D) effect, has been evaluated in case of four commercial steels via a series of heat treated conditions. The results have unequivocally established that the magnitude of S-D was maximum in the as quenched condition and tempering of the quenched structure led to a decrease in S-D. Spheroidised and/or annealed structures exhibited the lowest value of S-D. A linear relationship of S-D value with hardness and mean stress for each case has been established. Attempts have been made to explain the observed S-D effect in terms of models based on atomic mechanism and of continuum mechanics.

1. Introduction

The difference between compressive and tensile strength of a material at a given strain is termed as the strength differential (S-D). Theoretically the compressive and tensile strength of a material should be equal assuming that only shear stresses are responsible for plastic deformation and hydrostatic component of the stress system does not affect plastic flow [1]. However, in real materials like steels [2–36], zircaloy-2 [37–40], α (plutonium [41], dispersion strengthened alloys [42, 43], titanium alloys [44, 45], plastics [46], metal matrix compsosites [47, 48] and more recently in Ni Ti shape memory alloys [49, 50], a difference between the compressive and tensile strength is observed. Experimental evidence proves beyond doubt that the difference is genuine and cannot be accounted for merely as due to friction in the compression tests.

This phenomenon is gaining importance, as apart from providing theoretical curiosity, the S-D effect also has commercial relevance. In constructional steels, like beams, angles, channels etc., the members may often be subjected to high compressive loads. The choice of right microstructure to derive the maximum benefit from the S-D effect will reduce the quantity of metal used and thus reduce costs. In the aerospace industry, optimal exploitation of phenomenon can result in considerable savings in material costs. Another area is in nuclear reactor design to predict analytically the cladding creep collapse time during fuel densification for light water reactors [38, 39].

With reference to steels, most of the steels so far studied contain in addition to carbon a number of alloying additions. From a fundamental point of view it would be difficult to isolate the contribution to the total effect S-D from each of the alloying additions, in addition to the role of morphology and phase distribution.

In the present investigations, two plain carbon steels, differing in carbon content and two low alloy steels, essentially differing in nickel content have been considered. The study is mainly to conclude the role of carbon and nickel on the magnitude of S-D in identical experimental conditions. Contrary to most of earlier studies, the S-D effect has been evaluated at relatively larger strains of 1% offset and 10% true strain for different experimental conditions in case of all the four steels. Experimentally observed S-D values obtained under different experimental conditions have been analysed in terms of existing theories to explain the S-D phenomenon.

2. Experimental procedure

2.1. Materials, specimen preparation and heat treatment

The studied steels are two plain carbon and two low alloy steels, respectively named as A, B, C and D. The chemical compositions of these steels are given in Table I. These steels were received in the form of bars of 25.40 mm diameter. Cylindrical specimens of a constant diameter of 7.62 mm and different diameter to height ratios (D_0/H_0) of 1.00, 0.80 and 0.67 were machind from the bars for compression testing. Specimens of 25 mm gauge length and 6.25 mm diameter were machined from received bars for tensile tests.

Different heat treatments like brine quenching (Quenched in Sodium Chloride Solution), tempering,

* *Present Address*: Indian Institute of Technology, Kanpur, India.

† *Present Address*: Heavy Engineering Corporation, Ranchi, India.

TABLE I Chemical composition (wt.%) of steels

Steel	C	Mn	Si	Ni	Cr	Mo
A	0.17	0.70	0.21	—	—	—
B	0.80	0.67	0.19	—	—	—
C	0.34	0.60	0.17	1.80	1.24	0.32
D	0.34	0.61	0.16	3.9	1.20	0.30

spheroidising, normalising and annealing were employed in our investigations. Temperature and time for different heat treatments of all steels have been summarised in Table II.

Normalizing and annealing treatments for all the steels were given following the usual procedure. However, in case of normalising, instead of cooling in air, specimens were cooled in sand, to prevent oxidation. To prevent oxidation in the furnace vacuum sealing in silica tubes was employed in all the cases. The silica tube was broken before quenching from the temperature of austenitization.

The microstructure of the heat treated samples were examined by optical as well as scanning electron microscopy. They confirmed the desired microstructures achieved in each case.

2.2. Compression testing

On account of its higher load requirement, cylindrical specimens of all steels were compressed on a 30 tonne universal testing machine. A dial gauge having an accuracy of 2.5×10^{-3} mm was placed between the cross heads to record the displacement and hence the percent compression accurately. Compression tests were performed under constant cross-head speed. The initial strain rate obtained was $3.3 \times 10^{-4}\ s^{-1}$ for all the cases.

Frictionless true compressive stress was determined by employing the Cook and Larke technique [51]. In this technique, specimens of different initial diameter to height ratios, D_0/H_0, are compressed by a fixed strains e.g. 1%, 2%, 5%, 10% reduction in height. The observed stress, σ_{obs} is then plotted against the D/H values. While plotting the $\sigma_{obs} - (D/H)$ relationship, the strain was maintained constant for all the steels. Extrapolation to $D/H = 0$ gives the frictionless compressive stress for the given degree of compression. Here, D is the current diameter of the equivalent cylinder calculated from a constant specimen volume. H is the instantaneous height of the specimen estimated from the tool movement. Determination of frictionless compressive stress employing the Cook and Larke techique has been given in detail [52–56], though for other materials. Frictionless compressive stress, σ_c,—true strain (ε_t) curves were derived following the above procedure, for all the steels under different experimental conditions. The reported value of σ_c was an average of atleast three tests.

2.3. Tension testing

Room temperature tensile testing was conducted on a 5 tonne instron universal testing machine. Load elongation data obtained from the plotter were fed into a computer by points for determination of true stress(σ_T) true strain (ε_t) curves for all the steels. The initial strain rate was identical to those used for compression tests. The reported value of σ_T was an average of atleast three tests. A strain gauge extensometer was attached to the gauge length portion of the tensile specimen to measure the tensile strain accurately.

From the slope of the initial linear portion (elastic lines) of the stress strain curve, the Young's modulus of elasticity was evaluated for all the materials under different experimental conditions. The values obtained were $198 \times 10^3, 203 \times 10^3, 200 \times 10^3$ and 200×10^3 MPa for steels A, B, C and D respectively.

2.4. Hardness

The vickers hardness were measured using a 30 kg load for all the materials in different experimental

TABLE II Heat treatments for different steels

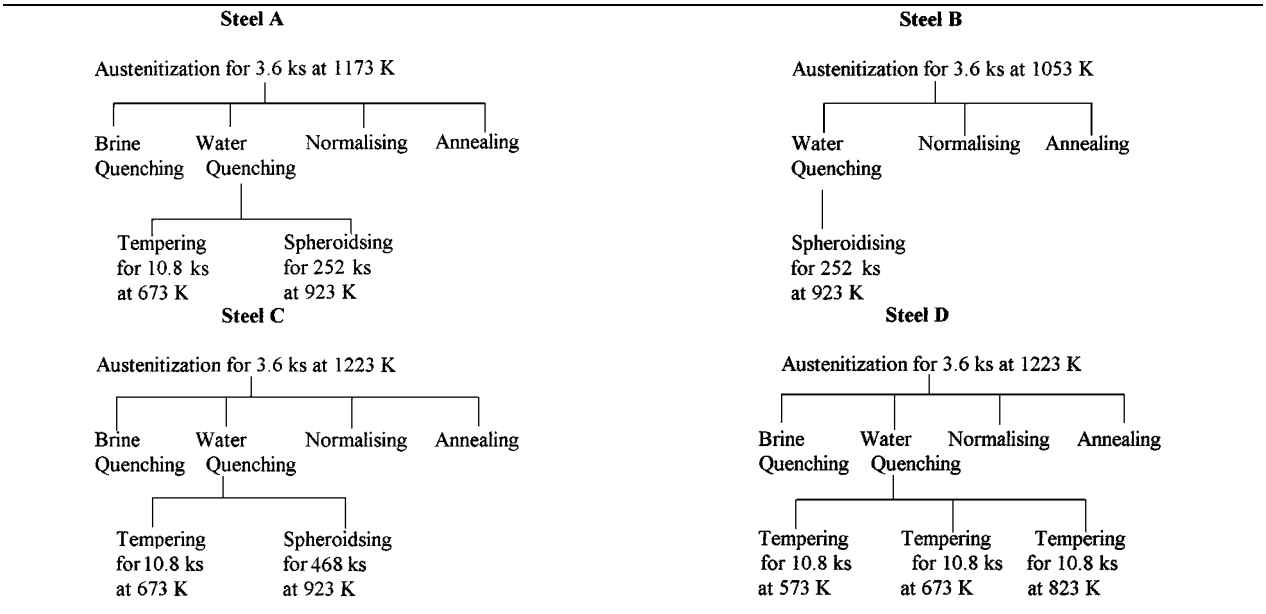

conditions. The reported values of the hardness were the average of 20 sets of measurements in each case.

2.5. Estimation of strengh differential effect

As a measure of strength differential effect, the % S-D was defined in two ways:

$$\%\text{S-D} = \frac{\sigma_c - \sigma_T \times 100}{\sigma_T} \quad (1)$$

$$\%\text{S-D} = \frac{\sigma_c - \sigma_T \times 100}{\sigma_m} \quad (2)$$

Where

$$\sigma_m = \frac{\sigma_c + \sigma_T}{2}$$

The final result for predicted % S-D by Pampillo and Coworkers [17, 18, 21, 25] for ferrous alloys is as follows:

$$\%\text{S-D} = \left[\frac{12\sigma_m}{E_0}(1 - 42\left(\frac{\sigma_m}{E_0}\right)^2\right] \times 100 \quad (3)$$

Where E_0 is the Young's modulus of elasticity at zero strain.

Spitzig-Richmond model [29] to predict S-D effect, based on pressure dependence of flow stress demonstrates that the flow stress, σ, depends linearly on hydrostatic pressure, p, in accord with the relation:

$$\sigma = \sigma_0(1 + 3\alpha p) \quad (4)$$

Where σ_0 is the value of σ at $p = 0$ (1 atmosphere) and is strain dependant, and α is a constant. To estimate the Probable S-D effect, Spitzig and Richmond plot a modified second stress invariant, I_2, against the first stress invariant I_1, the trace of the stress sensor. The second stress invariant, proportional to the effective stress is a measure of the driving force for plastic deformation. The first stress invariant is a measure of the hydrostatic stress. They have shown that there is a linear relationship between them:

$$I_2 = c - aI_1 \quad (5)$$

Where $I_1 = \sigma - 3p$, and $I_2 = \pm\sigma$ are stress invariants, a is a pressure coefficient and c is a strength coefficient. In Equation 5, σ is taken as positive in tension, and the sign for I_2 is taken so as to make the resultant value positive, that is, plus for tension, minus for compression. The coefficients a and c in Equation 5 are strain dependent. Substituting for I_1 and I_2 in Equation 5 results in the relation:

$$\sigma = \frac{c}{1 \pm a}\left(1 + 3\frac{a}{c}p\right) \quad (6)$$

Where the plus and minus sign in front of the coefficient a, are for tension and compression respectively. The quantity $c/1 \pm a$ is the value of σ when $p = 0$ (1 atmosphere) and is given the designation σ_0 in Equation 4. The coefficient ratio a/c is replaced by $\propto$ in Equation 4. $\propto$ is a constant, and like the elastic constant is a property of the bulk iron lattice [29]. $\propto$, has been found to have an average value of 19.2×10^{-6} MPa^{-1} for all iron based materials [29].

From Equation 6, it is possible to calculate the S-D, defined as the ratio of the difference between the absolute values of flow stress in tension and in compression to the average value. The magnitude of the strength differential is given by;

$$\%\,\text{S-D} = 2\left[\left(\frac{c}{1-a} - \frac{c}{1+a}\right)\Big/ \left(\frac{c}{1-a} + \frac{c}{1+a}\right)\right] \times 100 = 2a \times 100 \quad (7)$$

It is worth mentioning here that, superimposed hydrostatic pressure compression/tension tests have not been conducted in the present study. The value of 'a', was however, computed from the quantity $c/1 \pm a$ using compressive flow stress, σ_c, at the given strain.

$$\sigma_0 = \sigma_c = \frac{c}{1-a} \qquad \text{(In case of compression)}$$

$$\sigma_c \times \frac{a}{c} = \frac{a}{1-a} \qquad \text{(Multiplying both sides by } a\text{)}$$

$$1 + \alpha\sigma_c = 1 + \frac{a}{1-a} \quad (8)$$

(Adding 1 both sides and putting α for $\frac{a}{c}$)

$$a = \frac{\alpha\sigma_c}{1 + \alpha\sigma_c}$$

A constant value of 19.2×10^{-6} Mpa^{-1} for α was employed for all conditions.

3. Results

From the true compressive stress (σc)—true strain (ε_t) and true tensile stress (σ_T)—true strain (ε_t) curves, compressive and tensile flow stress at 1% offset and 10% true strain for steels A, B, C and D under different experimental conditions, were determined and are presented in Table IIIA–D respectively. Hardness (Hv) value obtained after each heat treatment for all the steels are also indicated in Table IIIA–D. True stress-true strain curves for compression along with tension under the entire range of strain studied, for the brine quenched and annealed condition in case of steel D are shown in Figs 1 and 2 respectively as examples.

Employing Equations 1, 2, 3 and 7, % S-D values were computed for all the steels under different experimental conditions. % S-D values determined from Equations 1 and 2 correspond to experimentally observed conditions, while values determined from Equations 3 and 7 model represent predicted conditions. Comparison of experimental S-D and model predictions are indicated in Figs 3a and b, 4a and b, 5a and b and 6a and b for steels A, B, C and D respectively.

TABLE IIIA Flow stress in compression and tension and vickers hardness value under different exerimental conditions for (a) Steel A, Initial strain rate 3.3×10^{-4} s^{-1}

Condition	Flow stress (MN m^{-2}) at 1% offset true strain		Flow stress) (MN m^{-2}) at 10% true strain		Hardness (Hv) 30 Kg. load
	σ_c	σ_T	σ_c	σ_T	
Brine quenched	1250	1085	1560	1350	397
Tempered for 10.8 ks at 673 K	640	620	930	900	280
Spheroidised	210	209	362	360	125
Normalised	290	287	445	440	184
Annealed	250	248	403	400	152

TABLE IIIB Steel B, Initial strain rate $= 3.3 \times 10^{-4}$ s^{-1}

Condition	Flow stress (MN m^{-2}) at 1% offset true strain		Flow stress (MN m^{-2}) at 10% true strain		Hardness (Hv) 30 Kg. load
	σ_c	σ_T	σ_c	σ_T	
Spheroidised	395	392	655	650	197
Normalised	525	518	810	800	268
Annealed	430	426.5	678	672	210

TABLE IIIC Steel C, Initial strain rate $= 3.3 \times 10^{-4}$ s^{-1}

Condition	Flow stress (MN m^{-2}) at 1% offset true strain		Flow stress (MN m^{-2}) at 10% true strain		Hardness (Hv) 30 Kg. load
	σ_c	σ_T	σ_c	σ_T	
Brine quenched	1470	1215	1790	1480	495
Tempered for 10.8 ks at 673 K	820	785	1150	1100	330
Spheroidised	300	298	444	440	187
Normalised	380	375	618	610	197
Annealed	330	327	480	475	189

TABLE IIID Steel D, Initial strain rate $= 3.3 \times 10^{-4}$ s^{-1}

Condition	Flow stress (MN m^{-2}) at 1% offset true strain		Flow stress (MN m^{-2}) at 10% true strain		Hardness (Hv) 30 Kg. load
	σ_c	σ_T	σ_c	σ_T	
Brine quenched	1600	1320	1930	1595	503
Tempered for 10.8 ks at 573 K	1020	960	1293	1220	362
Tempered for 10.8 ks at 673 K	870	830	1205	1150	336
Tempered for 10.8 ks at 823 K	610	595	905	880	280
Normalised	545	538	872	860	257
Annealed	450	445	647	640	202

% S-D values may be regarded as linearly decreasing functions of hardness (Hv) and mean stress (σm). Least square analysis has confirmed the linear relations observed S-D values appear to be nearly independent of strains. These relationships are indicated in Table IV at 1% offset true strain only. While establishing the linear relationship, % S-D values determined from Equation 2 have been considered.

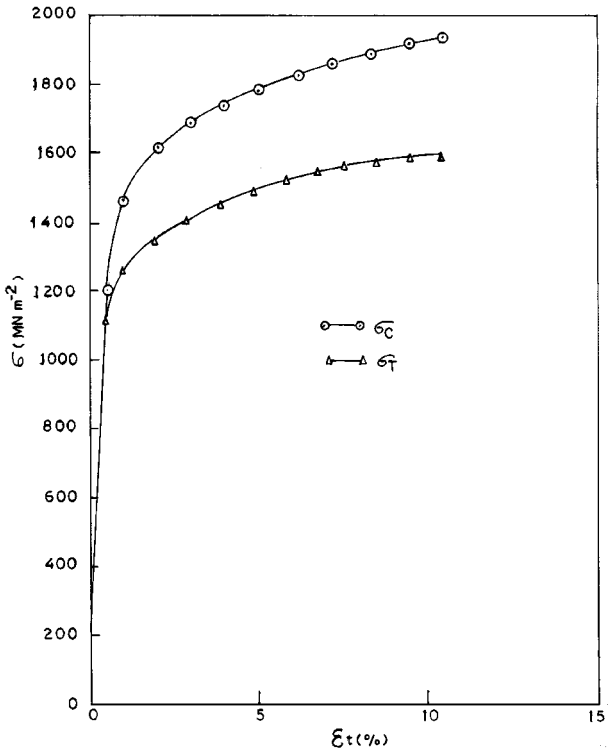

Figure 1 True stress true strain curves for compression and tension (Steel D, Brine quenched Condition).

4. Discussion

It was emphasized that for the S-D effect to consider genuine, the estimation of the same will have to be carried out at large strains [46]. The present theories of S-D [12, 17, 25, 29] also predicts its magnitude for large strains. In view of the above and also from our point of view, S-D effect corresponding to relatively higher strains of 0.01 (1% true strain) and 0.10 (10% true strain), has been estimated for all the steels. Persistence of this phenomenon to very large strains clearly indicate that this effect is real (Figs 3a and b, 4a and b, 5a and b and 6a and b).

S-D effect has been expressed as a percentage of the tensile flow stress or as the percentage of the average of compressive and tensile flow stresses at the given strain. The former has practical significance, because in industrial situations, considerations of material saving will require a knowledge of the gain in strength over and above the tensile strength. On the other hand, a theoretical understanding of the phenomenon of S-D effect [12, 17, 25, 29] will require that the difference between the compressive and tensile flow stresses is expressed as a percentage of the mean flow stress. On account of this in the present case the S-D was expressed in both ways.

Experimental results in our case revealed that the magnitude of S-D is maximum for the as brine quenched condition and there is a decrease in value of S-D with increasing tempering temperature is in agreement with the findings of other authors [11, 14, 15, 27]. The fact that a total elimination of S-D occurs only when

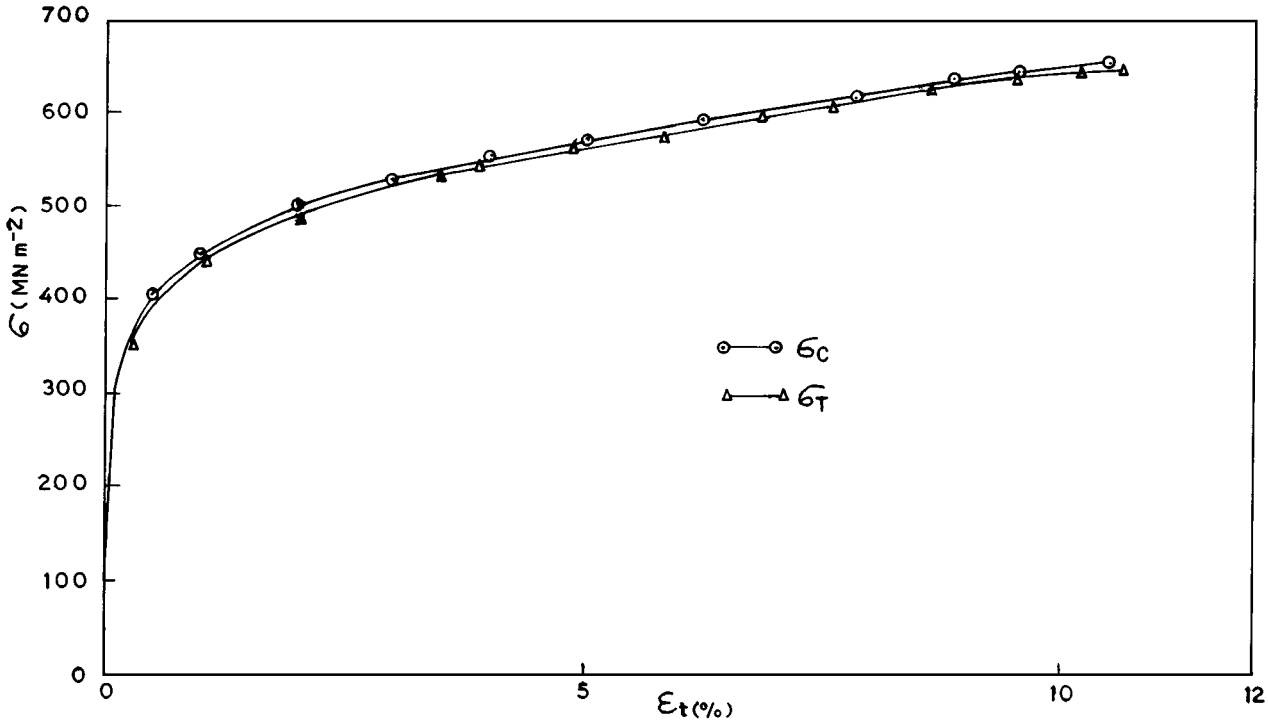

Figure 2 True stress true strain curves for compression and tension. (Steel D, Annealed condition).

TABLE IV Equations relating Hardness (Hv), Mean stress (σ_m) and S-D (%) at 1% offset true strain

Steel grade	Equation	Correlation
A	SD (%) = 0.0485 × Hv − 7.114	0.8659
	SD (%) = 0.0139 × σ_m − 3.162	0.9418
B	SD (%) = 0.0083 × Hv − 0.889	0.998
	S-D (%) = 0.0047 × σ_m − 1.125	0.9816
C	S-D (%) = 0.056 × Hv − 10.390	0.9265
	S-D (%) = 0.0168 × σ_m − 5.323	0.9221
D	S-D (%) = 0.062 × Hv − 14.267	0.9068
	S-D (%) = 0.0175 × σ_m − 8.452	0.9209

the tempering of the quenched product (martensile) is carried out at a temperature above the recrystallization range for the material is also nearly valid for our investigations (Figs 3a and b, 4a and b, 5a and b and 6a and b). The absence of S-D in an annealed condition reported earlier [15] is also in close agreement with our findings.

The earlier results [9, 12] that there is an increase in the value of S-D with increasing carbon content in the identical quenched/tempered conditions could not be validated as in case of steel B, the tensile specimens corresponding to the brine Quenched and tempered conditions failed in the grip region. However, for other conditions, e.g. spheroidising, normalising and annealing, the magnitude of S-D has been influenced by carbon content, though to a lesser extent.

The magnitude of S-D observed for both steel C and D under identical conditions indicate that nickel is perhaps unimportant in influencing the magnitude of S-D.

The presence of significant S-D at large strains in the present case eliminates micro-cracking, residual stresses and retained austenite hypotheses as the major reasons for the occurence of the phenomenon of S-D effect. Detailed justification for this stand has also been given [11, 14, 15]. Likewise, the occurence of S-D at large strains also eliminates the Internal Bauschinger effect arising from the presence of compressive stresses accompanying the formation of martensile. The conventional Bauschinger effect that may be present on account of the prior thermomechanical history as a source of S-D is ruled out completely. Volume expansion occuring during plastic deformation in a tensile or compression test could account for the S-D effect. Such an expansion would influence the yield criterion causing the flow stress in uniaxial compression to be greater than the flow stress in uniaxial tension. The adequacy of the volume change explanation for the S-D in steel depends on whether the actual expansion versus strain is of sufficient magnitude and also whether it takes place during the rate controlling event of the deformation process. It has been reported [29, 31] that the observed plastic volume change which is in accord with expected increase in dislocation density, is negligible by comparison with that predicted by the normality flow rule [57]. However, volume change determinations resulting from plastic deformation have not been made, in the present study.

The most discussed model for the phenomenon based on atomic mechanism is due to Hirth and Cohen [12]. According to this model, severe lattice distortion arising on quenching produces non-linear elastic fields leading to a greater binding energy between carbon atoms and dislocations in case of compression compared to tension. This would require S-D to be highest in the quenched condition which is indeed the case. In this approach, therefore, as tempering leads to a reduction in the severity of lattice distortion, it should lead to a decrease in the magnitude of S-D which again is verified by experimental results (Figs 3a and b, 4a and b, 5a and b and 6a and b). The reduction in S-D with increase in

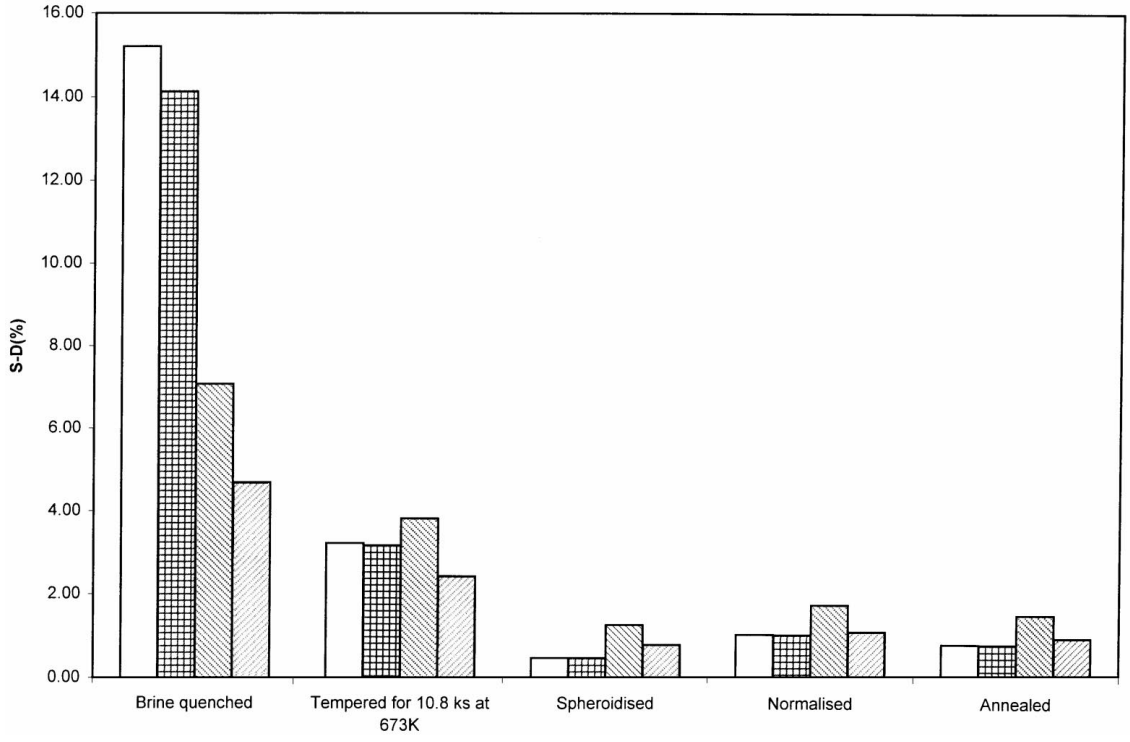

(a)

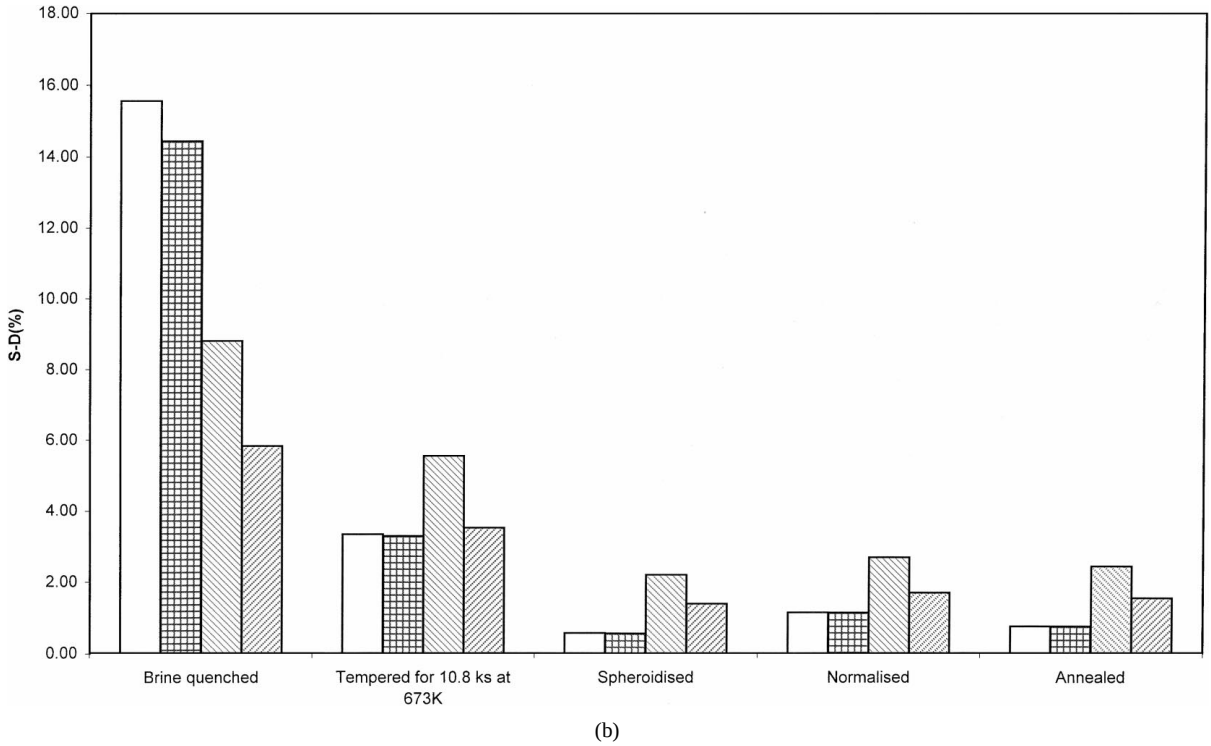

(b)

Figure 3 Comparison of the experimental S-D and the model predictions for Steel A (a) 1% offset true strain (b) 10% true strain. (□) Experimental (Equation 1), ▦ Experimental (Equation 2), ▧ Pampillo and Coworkers model, ▨ Spitzig–Richmond model.

tempering temperature in case of steel D is also in agreement with the model [12]. The effect of the increasing tempering/spheroidising temperature is to reduce the severity of lattice distortion and hence S-D. The observation of low value of S-D in the annealed condition is reasonable because the ferrite pearlite structure obtained in the annealed condition is closest to the ideal equilibrium isotropic structure. As, an ideal isotropic structure will possess similar strength values in all directions, it is understandable that the S-D in this case is very small. The slightly higher value of S-D obtained in case of normalising compared to annealing may be due to a difference in cooling rate after austenitization. However, this theory can only predict a maximum S-D of about 6% in the hardened condition. This is clearly insufficient to account for the present results. The near absence of S-D in the annealed condition cannot be accounted satisfactorily by this model. Thus a qualitative understanding of the present results is possible in terms of this model [12].

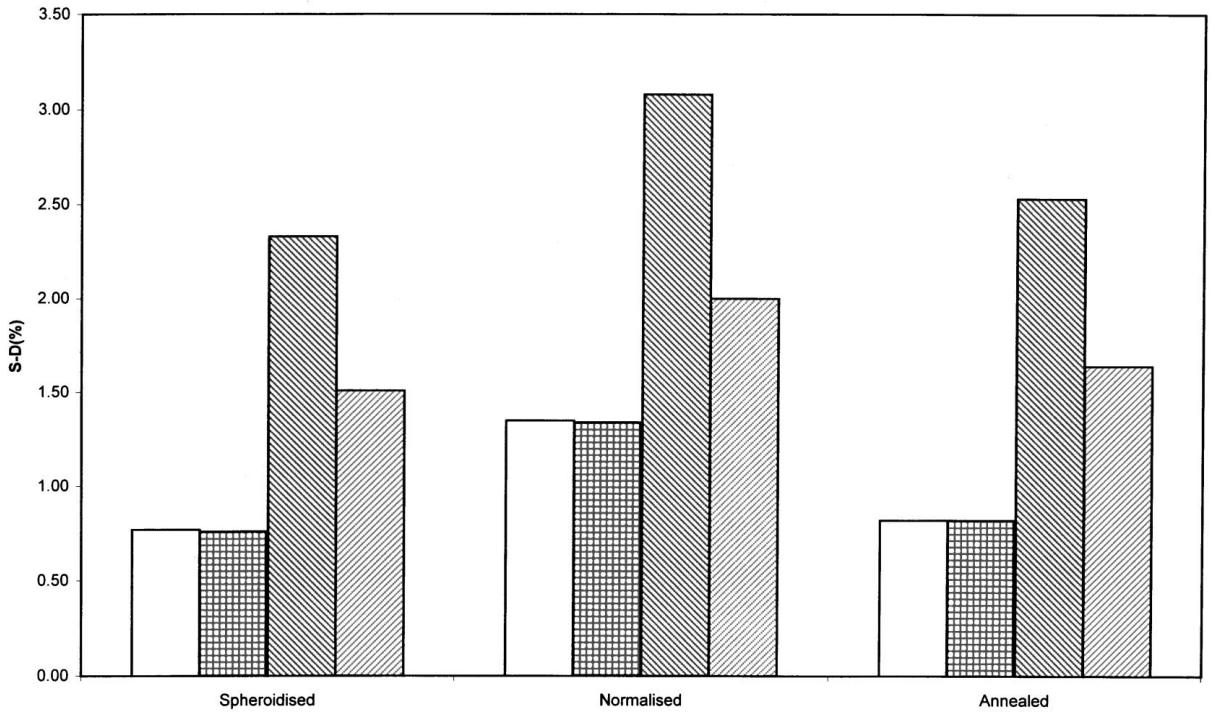

(a)

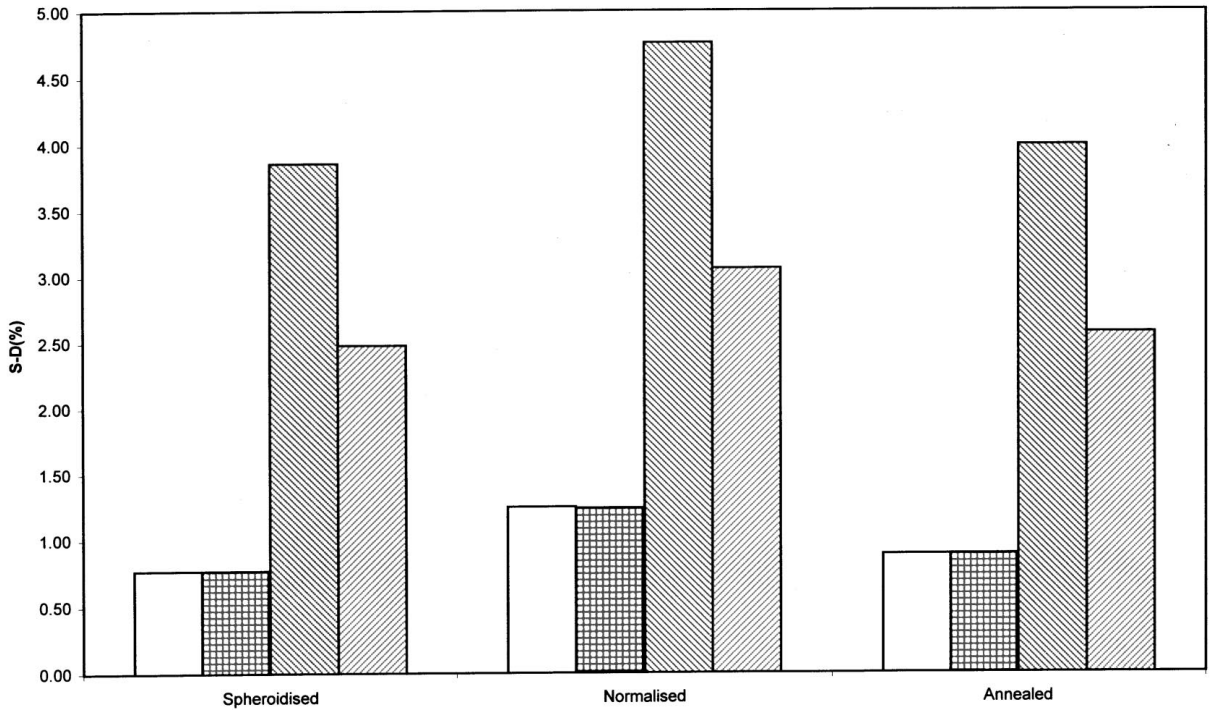

(b)

Figure 4 Comparison of the experimental S-D and the model predictions for Steel B (a) 1% offset true strain (b) 10% true strain, key same as in Fig. 3.

Modified version of Hirth and Cohen's non linear approach is a model by Pampillo and co-workers [17, 19, 21, 25]. They considered the flow stress to be made of an internal stress σ_i, due to the interactions of the dislocations with long range stress field, and an effective stress, σ^*, which is assumed to be negligible at room temperature for both quenched and quenched and tempered conditions. At sufficiently large elastic strains, the elastic modulus does not remain constant but depends on the strain in such a way that it is smaller in tension than in compression. In such a case, it can be predicted that the S-D effect is simply due to an increase of σ_i during compression and a decrease of σ_i during tension, due to a change in elastic modulus.

Prediction of Pampillo and co-workers (Figs 3a and b, 4a and b, 5a and b and 6a and b) gives good agreement with experimental results especially for quenched condition compared to Hirth and Cohen's model [12]. In a clear right trend S-D is predicted for tempered and other conditions, but observed S-D values decrease faster with decreasing mean stress (σ_m) or hardness value than predicted. Decrease of observed S-D values

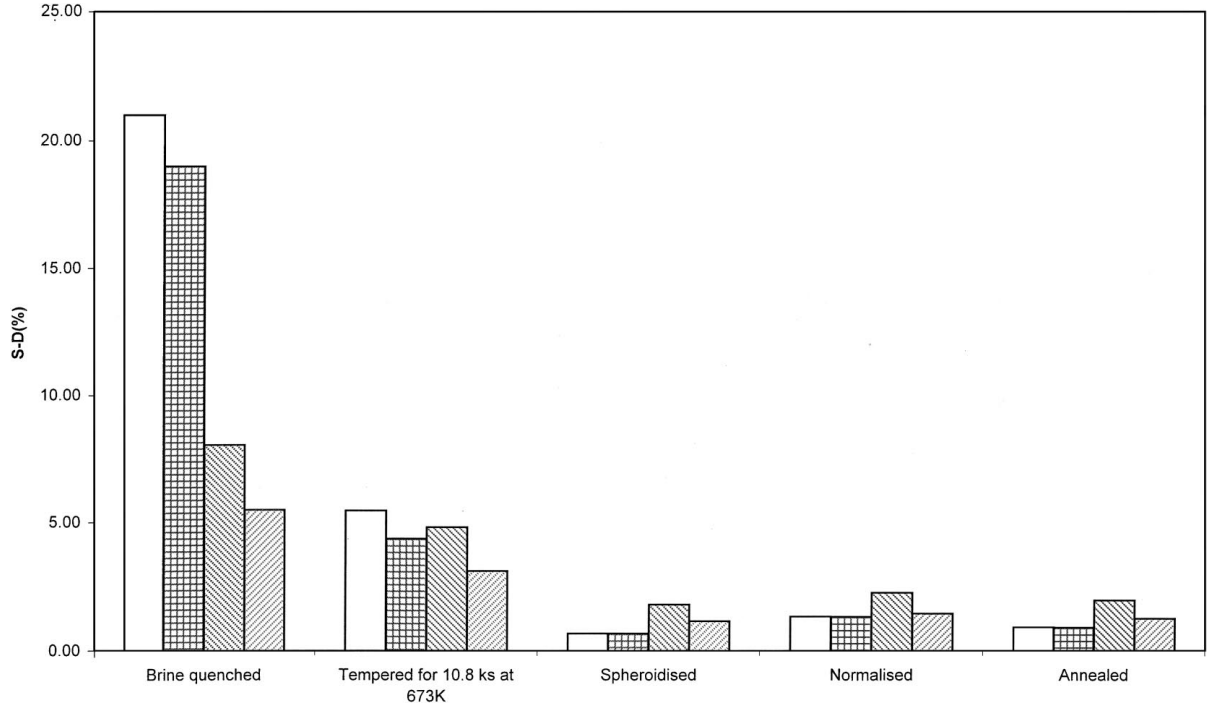

(a)

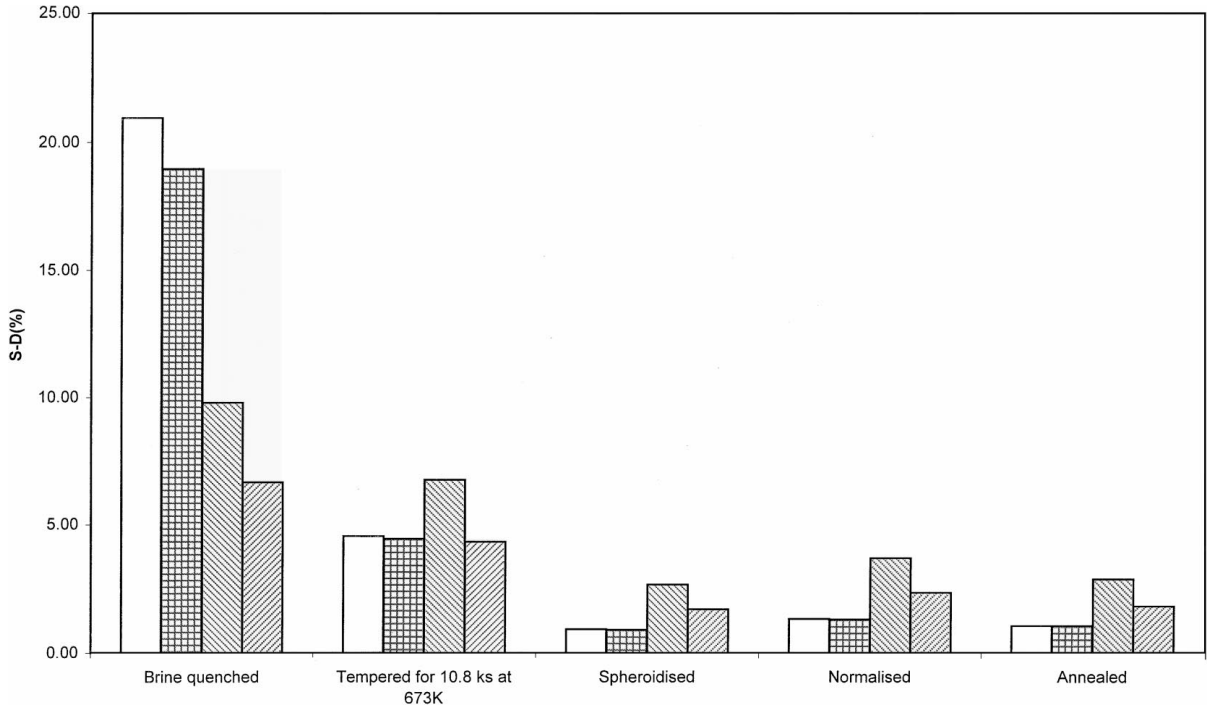

(b)

Figure 5 Comparison of the experimental S-D and the model predictions for Steel C (a) 1% offset true strain (b) 10% true strain, key same as in Fig. 3.

with decreasing mean stress (σ_m) is in line with the model. However, this model also fails to explain our results quantitatively.

The Spitzig Richmond model [29] based on continuum mechanics, basically demonstrates that the S-D effect is a natural extension of the effect of pressure dependance of the flow stress measured under high hydrostatic pressure, extended to the level of variation in the hydrostatic stress between tensile and compression tests at ambient pressure. This pressure dependence is in general agreement with the effect of the atomic bond asymmetry on the stress required to move a dislocation through the lattic [29, 58].

Results on S-D (Figs 3a and b, 4a and b, 5a and b and 6a and b) indicate clearly a relatively better agreement compared to other models between the predicted values from Spitzig-Richmond's model and the experimentally observed values, except in the quenched condition. The variation in observed S-D values with experimental conditions, are also in line with the model,

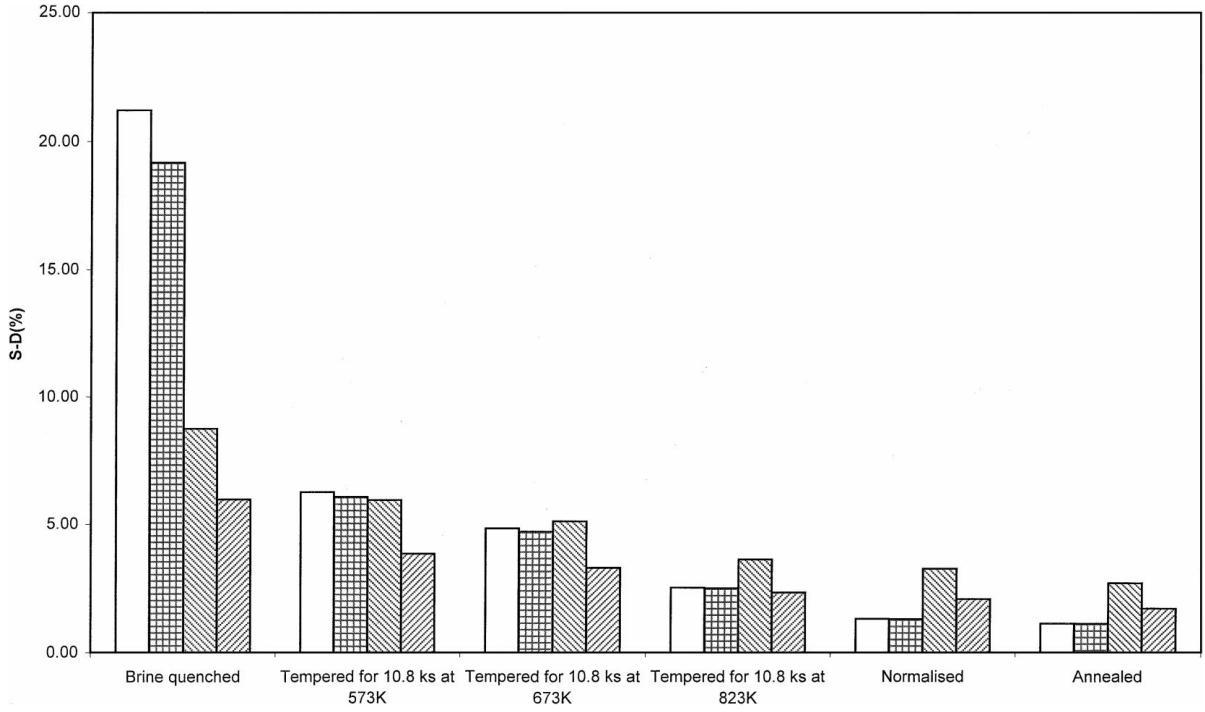

(a)

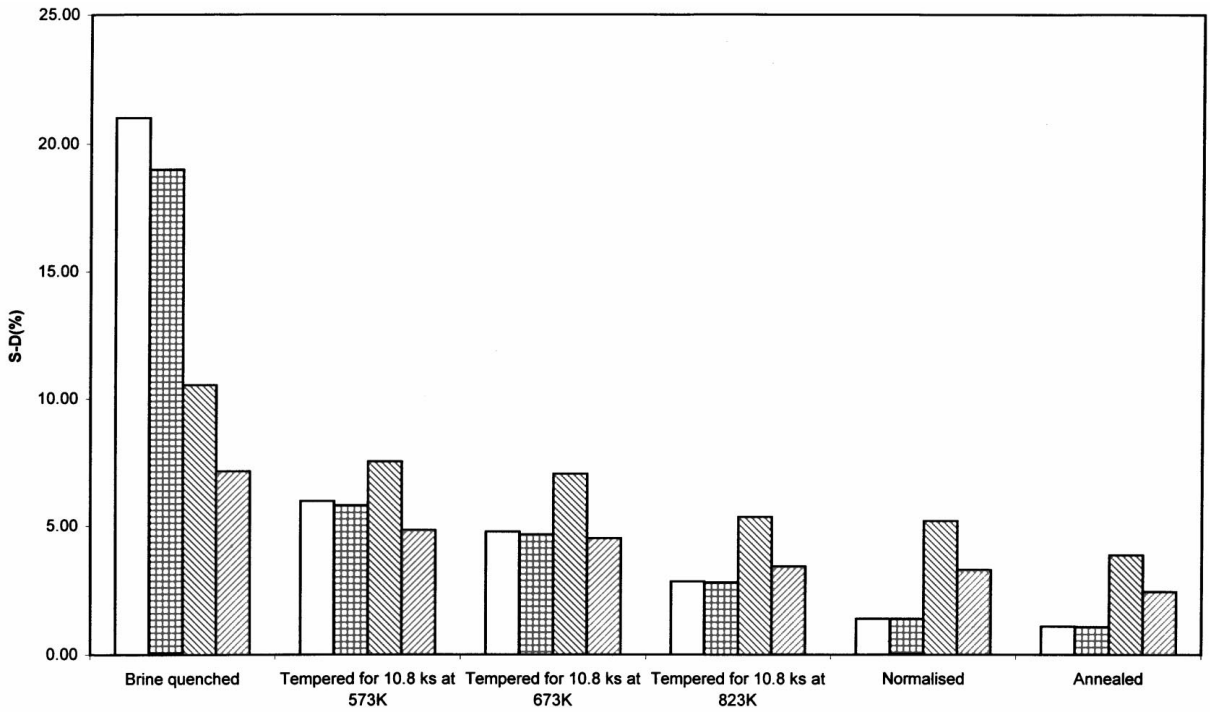

(b)

Figure 6 Comparison of the experimental S-D and the model predictions for Steel D (a) 1% offset true strain (b) 10% true strain, key same as in Fig. 3.

on the basis that there is a linear relationship of '*a*' with strength coefficient *c* (representative of strength or hardness of a material). Agreement at lower strain (1%) is better. This is understandable, as '*a*' is strain dependent and observed S-D values appear to be independent of strains.

It is evident from above that none of the theories [12, 17, 25, 29] are able to explain quantitatively the observed phenomenon of S-D effect. Spitzig-Richmond's model however, gives relatively better agreement for most of our observations, except in the quenched condition.

5. Conclusions

The strength differential effect has been evaluated in case of four commercial steels via a series of heat treated conditions. The studies led to the following conclusions:

i) The as untempered martensitic structure leads to the largest value of S-D.

ii) Tempering of martensitic structure leads to a decrease in S-D and there is a decrease in S-D value with increase in tempering temperature.

iii) Annealed as well as spheroidised structures lead to a very low value of S-D.

iv) Nickel seems to be perhaps unimportant in determining the level of S-D in a given material.

v) An increase in the carbon content increases the magnitude of S-D.

vi) A linear relationship of S-D value with hardness and mean stress values for each case has been established.

vii) Pressure dependence flow stress model due to Spitzig and Richmond appears most promising among the existing theories as this gives relatively better agreement with most of the experimental observations.

References

1. P. W. BRIDGMAN, "Studies in Large Plastic Flow and Fracture" (Mc Grraw Hill, New York, 1952).
2. J. BAUSCHINGER, *Mitt Mech-Tech. Lab. Munchen* **13** (1886) 1 (Cited by S. N. BUCKELY and K. M. ENTWISTLE, *Acta. Met.* **4** (1956) 352.
3. E. SIEBEL and A. POMP, *Mitteilungen Kaiser Wilhelm Inst. Eisenforschung* **9** (1927) 157.
4. *Idem., ibid.* **10** (1928) 55.
5. N. H. POLAKOWSKI, *J. Iron Steel Inst.* **163** (1949) 250.
6. F. GAROFALO and H. A. WRIEDT, *Acta Met.* **10** (1962) 1007.
7. H. CONRAD, *Trans ASM* **57** (1964) 747.
8. A. R. ROSENFIELD and G. T. HAHN, *ibid.* **59** (1966) 962.
9. W. C. LESLIE and R. J. SOBER, *ibid.* **60** (1967) 99, 459.
10. G. R. SPEICH, Seminar on the Strength Diffrential Effect in Martensile, U.S. Steel Corporation, 1968.
11. D. KALISH and M. COHEN, *Trans. ASM* **62** (1969) 353.
12. J. P. HIRTH and M. COHEN, *Met. Trans.* **1** (1970) 3.
13. *Idem., J. Met.* **21** (1969) 27.
14. R. CHAIT, *Met. Trans.* **3** (1972) 365.
15. D. C. RAUCH and W. C. LESLIE, *ibid.* **3** (1972) 373.
16. D. KALISH and H. J. RACK, *ibid.* **3** (1972) 2289.
17. C. A. PAMPILLO, L. A. DAVIS and J. C. M. Li, *Scripta Met.* 6 (1972) 765.
18. W. C. LESLIE, *ibid.* **6** (1972) 1145.
19. *Idem., ibid.* **6** (1972) 1147.
20. N. LOUT and J. M. GALLIGAN, *ibid.* **7** (1973) 253.
21. C. A. PAMPILLO, L. A. DAVIS and J. C. M. LI, *ibid.* **7** (1973) 255.
22. K. TANAKA and T. MORI, *ibid.* **7** (1973) 307.
23. R. CHAIT, *ibid.* **7** (1973) 351.
24. N. LOUT and J. M. GALLIGAN, *ibid.* **8** (1974) 581.
25. C. A. PAMPILLO, L. A. DAVIS and J. C. M. LI, *ibid.* **8** (1974) 685.
26. I. B. FLETCHER, M. COHEN and J. P. HIRTH, *Met Trans.* **5** (1974) 905.
27. P. N. THIELEN and M. E. FINE, *Scripta Met.* **9** (1975) 383.
28. Y. DUBOC DO NATAL and S. N. MONTERIRO, *Metal A B M* **33** (1977) 269.
29. W. A. SPITZIG and O. RICHMOND, *Acta Met.* **32** (1984) 457.
30. G. C. ROUCH, R. L. DAGA, S. V. RADCLIFFE, R. J. SOBER and W. C. LESLIE, *Met. Trans.* **6** (1975) 2279.
31. W. A. SPITZIG, R. J. SOBER and O. RICHMOND, *Acta Met.* **23** (1975) 895.
32. *Idem., Met. Trans.* **7** (1976) 1703.
33. W. A. SPITZIG, *Acta Met.* **27** (1978) 523.
34. D. F. WATT and M. JAIN, *Scripta Met.* **18** (1984) 1379.
35. D. R. DRYDEN, D. F. WATT, *ibid.* **20** (1986) 1727.
36. D. J. KIM and S. W. NAM, *ibid.* **21** (1987) 1121.
37. S. L. MANNEN and P. RODRIQUEZ, *ibid.* **5** (1971) 710.
38. G. E. LUCAS and A. L. BEMENT, *J. Nucl. Met.* **55** (1975) 246.
39. *Idem., ibid.* **58** (1975) 163.
40. D. G. FRANKLIN, *ibid.* **58** (1975) 361.
41. M. D. MERZ, *Met. Trans.* **4** (1973) 1186.
42. R. J. OLSEN and G. S. ANSELL, *Trans. ASM* **62** (1969) 711.
43. LESZYNSKI, "Powder Metallurgy" (Interscience, New York, 1961) p. 306.
44. M. R. WINSTONE, M. L. RIGHT and R. D. RAWLINGS, *Scripta. Met.* **7** (1973) 1265.
45. M. A. LOWDEN and W. B. HUTCHINSON, *Met. Trans.* **6** (1975) 441.
46. D. C. DRUCKER, *ibid.* **4** (1973) 667.
47. R. J. ARESENAULT and M. TAYA, *Acta Met.* **35** (1987) 651.
48. R. J. ARSENAULT and S. B. WU, *Mater Sci. Engg.* 96 (1987) 77.
49. R. PLIETSCH and K. EHRLICH, *Acta Mater.* **45** (1997) 2417.
50. Y. LIU, Z. XIE, J. VAN HUMBECK and L. DELAEY, *ibid.* **46** (1998) 4325.
51. M. COOK and E. C. LARKE, *J. Inst. Met.* **71** (1945) 371.
52. K. A. PADMANABHAN, Ph.D thesis, University of Cambridge, 1971.
53. K. A. PADMANABHAN and G. J. DAVIES, *Met. Sci.* **11** (1977) 177.
54. G. J. RICHARDSON, D. N. HAWKINS and C. M. SELLARS, "Worked Examples in Metal Working" (The Institute of Metals, London, 1985) p. 13.
55. A. P. SINGH and K. A. PADMANABHAN, *J. Mater. Sci.* **26** (1991) 5481.
56. *Idem., ibid.* **26** (1991) 5488.
57. R. VON MISES and Z. ANGEW, *Math. Mech.* **8** (1928) 161.
58. J. JUNG, *Phil. Mag.* **43** (1981) 1057.

Received 19 February
and accepted 30 September 1999